Quantum Simulations of Hadronic Systems

Diogo Cruz
diogo.da.silva.duarte.cruz@tecnico.ulisboa.pt

Instituto Superior Técnico, Lisboa, Portugal

October 2019

Abstract

In this work, we propose a new methodology to study physical systems in QCD with quantum computers, that uses the hybrid classical-quantum algorithm known as the Variational Quantum Eigensolver (VQE). Starting from a QCD-inspired Hamiltonian, we derive an effective Hamiltonian that satisfies both confinement and chiral-symmetry requirements. We later show that the previous Hamiltonian can be *translated* to an equivalent problem of several interacting spins, by means of a Bravyi-Kitaev transformation. Within its simplest approximation, requiring only 2 *qubits*, we reproduce the mass spectrum of vector mesons, within an approximation where no particular interquark potential needs to be assumed. Even though these results could easily be obtained with classical computers, they represent a first step towards a systematic implementation for similar quark-composite systems. Our method is also applicable to arbitrary fermionic bound-state systems. For more complex systems, we present a new general method for simplifying the implementation of the VQE algorithm.
Keywords: hadronic systems, variational quantum eigensolver (VQE), quantum circuit, mesonic states, state preparation

1. Introduction

Nowadays, an outstanding issue in Quantum Chromodynamics (QCD) remains: how to treat its non-perturbative nature in the low energy regime. This is the regime characteristic of the physical systems in QCD, namely all the building blocks of ordinary matter: the nucleons (protons and neutrons), as well as other hadronic bound states (mesons and baryons) and the exciting exotic states thereof (tetraquarks, glueballs, hybrids, etc.).

Over the years though, a large number of theoretical models describing quarks in hadronic bound states have been proposed. However, the full effect of quark-antiquark pairs has never been considered. This is because such effects lead to a many-body problem that can only be treated in some approximation, and quite often requiring huge computational effort.

Interestingly, after Quantum Computing was shown to be able to surpass the capabilities of its classical counterparts, a boom in research in this field has been observed.

In this context, a new algorithm has been introduced, the Variational Quantum Eigensolver (VQE, see [1]). By combining classical and quantum computation, this hybrid algorithm has shown to be robust to noise in quantum hardware, and has opened the possibility of studying, in the near future, physical systems currently out of reach by classical methods alone. It has been used extensively in Quantum Chemistry, however, on the field of QCD, research has been far more limited. An example is considered in ref. [2], in which lattice gauge theories, such as lattice QCD, have been transcribed to Hamiltonians composed of Pauli operators, so that they can be computed on quantum hardware. The analysis was purely theoretical, and the method suggested to obtain the energy spectrum was quantum phase estimation. Unfortunately, quantum phase estimation demands fully coherent evolution (see [1]), as it is not robust to errors. Since it uses an evolution operator decomposed through trotterization, its implementation requires a significant number of quantum gates applied in succession, so current quantum hardware would only be powerful enough to implement very simple physical systems.

It is important to emphasize that whatever model/approximation to QCD one favours to address hadronic states, it should obey three conditions:

- It has to "contain" confinement,
- It has to be chiral symmetric and, despite that,
- possess a mechanism for spontaneous breaking of chiral symmetry (SχSB).

There is a class of models which can address, at one stroke, all the three above conditions: they are chiral symmetric, they display SχSB, and, on top, they allow for chiral restoration. This class of models (see Eq. 1 where the QCD-inspired Hamiltonian is introduced), can be thought as to solve QCD

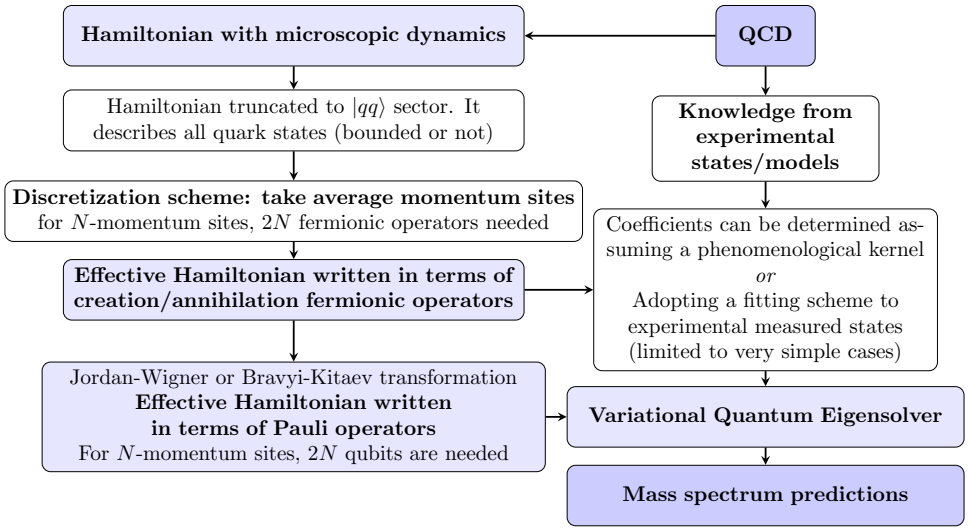

Figure 1: Schematic overview of the steps needed in order to simulate hadronic states with quantum processors. The method is illustrated for the case of mesons, but it could easily be extended to other systems.

in the Gaussian approximation for gluonic cummulants. This approximation becomes exact in the limit of heavy quarks, and it is the starting point of the methodology hereby proposed. A schematic overview of the method is shown in Fig. 1.

The second step amounts to construct a new effective Hamiltonian written in terms of fermionic creation/and annihilation operators acting on an abstract qubit space. The key idea is to consider average momentum sites for both species of particles (the quark and antiquark).

There are different ways in which this can be done. In quantum electronic problems of molecules, for example, each fermionic operator is associated with the creation/annihilation of one electron in one quantum orbital. The strategy used here is slightly different. Instead, average momentum sites for both species of particles (quark and antiquark) are considered. As it will be shown further in this document, by choosing only two of these momentum 'sites', it is possible to retain all relevant interactions.

Finally, the Bravyi-Kitaev transformation is used to map the latter Hamiltonian into one that is composed of Pauli operators, in order to be computed on quantum hardware, using the IBM Quantum Experience (see [3]). This way, the cost of this encoding (no error correction qubits included) is $2N$ qubits, for N-momentum sites.

In this study, the simplest approximation of $N = 2$ momentum sites is used to simulate with the IBM quantum processors *ibmq_16_melbourne* and *ibmq_ourense* the mass spectrum of vector mesons. For these systems, the available experimental results and some estimated guesses are considered to fit the coefficients of our model.

This paper is organised as follows: Sec. 2 introduces the QCD formalism, followed by Sec. 3 and Sec. 4 where the effective Hamiltonian and the Bravyi-Kitaev transform are presented. Sec. 5 contains the quantum computing results and Sec. 6 introduces a new procedure for state preparation in the VQE algorithm. Sec. 7 presents the conclusions.

2. Formalism

2.1. Hamiltonian model

In this work, we restrict ourselves to the quark sector, and assume an implicit phenomenological kernel, that, as we show later in this paper, we *will not* need to specify.

Thus, we obtain a much simpler Hamiltonian that nevertheless contains all the relevant microscopic quark physics. This effective Hamiltonian has been previously introduced in ref. [4]:

$$H_{\text{eff.}} = \int d\boldsymbol{x}\bar{\psi}(\boldsymbol{x},t)\overbrace{(-i\boldsymbol{\alpha}\cdot\boldsymbol{\nabla}+\beta m)}^{\mathcal{K}}\psi(\boldsymbol{x},t) - \frac{1}{2}\int d\boldsymbol{x}d\boldsymbol{y}\rho^a_\mu(\boldsymbol{x},t)\mathcal{V}^{ab}_{\mu\nu}(\boldsymbol{x}-\boldsymbol{y})\rho^b_\nu(\boldsymbol{y},t) \quad (1)$$

where ψ is the current bare quark field, m is the bare mass, and

$$\rho^a_\mu(\boldsymbol{x},t) = \bar{\psi}(\boldsymbol{x},t)\gamma_\mu\frac{\lambda^a}{2}\psi(\boldsymbol{x},t) \quad (2)$$

is the color density, parametrised through an instantaneous quark kernel,

$$\mathcal{V}^{ab}_{\mu\nu}(\boldsymbol{x}-\boldsymbol{y}) = g_{\mu 0}g_{\nu 0}\delta^{ab}V_0(|\boldsymbol{x}-\boldsymbol{y}|) \quad (3)$$

Using a plane wave spinor expansion for the quark field with a given *flavor (f)* and *color (c)*, one can write (see [4, 5, 6]):

$$\psi_{fc}(\boldsymbol{x},t) = \sum_s\int\frac{d\boldsymbol{k}}{(2\pi)^3}[u_s(\boldsymbol{k})b_{fcs}(\boldsymbol{k})e^{-ik_0t} + v_s(\boldsymbol{k})d^\dagger_{fcs}(-\boldsymbol{k})e^{ik_0t}]e^{i\boldsymbol{k}\cdot\boldsymbol{x}} \quad (4)$$

where u_s and v_s are free particle, antiparticle

spinors, and $b^\dagger_{fcs}(b_{fcs})$ and $d^\dagger_{fcs}(d_{fcs})$ correspond to creation (annihilation) operators of bare quarks and antiquarks, respectively.

$\psi_{fc}(\boldsymbol{x},t)$ can be expanded in a new quasiparticle basis (being left to the actual interaction to determine which must be the appropriate basis):

$$\psi_{fc}(\boldsymbol{x}) = \sum_s \int \frac{d\boldsymbol{k}}{(2\pi)^3}[U_s(\boldsymbol{k})B_{fcs}(\boldsymbol{k}) + V_s(\boldsymbol{k})D^\dagger_{fcs}(-\boldsymbol{k})]e^{i\boldsymbol{k}\cdot\boldsymbol{x}} \quad (5)$$

entailing quasiparticle spinors U_s and V_s and operators B_{fcs} and D_{fcs}. The Hamiltonian is equivalent in either basis and the two are related by a similarity (Bogoliubov-Valatin of BCS) transformation. This corresponds to the following rotation in terms of the BCS angle $\theta_k \equiv \theta(k)$ and $\varphi_k = 2\theta_k + \arctan(m/k)$:

$$\begin{aligned}
B_{fcs}(\boldsymbol{k}) &= \cos(\theta_k)b_{fcs}(\boldsymbol{k}) - s\sin(\theta_k)d^\dagger_{fcs}(-\boldsymbol{k}) \\
D_{fcs}(-\boldsymbol{k}) &= \cos(\theta_k)d_{fcs}(-\boldsymbol{k}) + s\sin(\theta_k)b^\dagger_{fcs}(\boldsymbol{k}) \\
U_s(\boldsymbol{k}) &= \frac{\left(1+\sin(\varphi_k)\beta + \cos(\varphi_k)\boldsymbol{\alpha}\cdot\hat{\boldsymbol{k}}\right)u_{0,s}}{\sqrt{2(1+\sin(\varphi_k))}} \\
V_s(\boldsymbol{k}) &= \frac{\left(1-\sin(\varphi_k)\beta - \cos(\varphi_k)\boldsymbol{\alpha}\cdot\hat{\boldsymbol{k}}\right)v_{0,s}}{\sqrt{2(1+\sin(\varphi_k))}} \quad (6)
\end{aligned}$$

where $u_{0,s}$ and $v_{0,s}$ stand respectively for the rest spinors of quarks and antiquarks.

2.2. From time ordering to normal ordering

From the Hamiltonian of Eq. 1 we use the Wick theorem to write down a normal ordered Hamiltonian (see [4]):

$$\begin{aligned}
H &= H_0 + :H_2: + :H_4: \\
H_0 &= \overbrace{\psi^\dagger\mathcal{K}\psi} + \overbrace{\psi^\dagger\Gamma\overbrace{\psi\mathcal{V}\psi^\dagger}\Gamma\psi} \\
H_2 &= \psi^\dagger\mathcal{K}\psi + \psi^\dagger\Gamma\overbrace{\psi\mathcal{V}\psi^\dagger}\Gamma\psi + \overbrace{\psi^\dagger\Gamma\psi\mathcal{V}\psi^\dagger\Gamma\psi} \\
H_4 &= \psi^\dagger\Gamma\psi\mathcal{V}\psi^\dagger\Gamma\psi \quad (7)
\end{aligned}$$

Performing the Wick contractions, marked with upper square brackets, we obtain:

$$\begin{aligned}
H_0 &= -3N_f\int\frac{d\boldsymbol{x}}{(2\pi)^3}\int d\boldsymbol{k}\left[-\frac{2}{3}C(\boldsymbol{k}) + E(\boldsymbol{k}) + m\sin\varphi_k + \boldsymbol{k}\cos\varphi_k\right] \quad (8) \\
H_2 &= H_2^A + \int d\boldsymbol{k}E(\boldsymbol{k})\left[B^\dagger_{fcs}(\boldsymbol{k})B_{fcs}(\boldsymbol{k}) + D^\dagger_{fcs}(\boldsymbol{k})D_{fcs}(\boldsymbol{k})\right] \quad (9) \\
A(\boldsymbol{k}) &\equiv m + \frac{2}{3}\int d\boldsymbol{k}'V(\boldsymbol{k}-\boldsymbol{k}')\sin\varphi_{k'} \\
B(\boldsymbol{k}) &\equiv \boldsymbol{k} + \frac{2}{3}\int d\boldsymbol{k}'V(\boldsymbol{k}-\boldsymbol{k}')\cos\varphi_{k'}\,\hat{\boldsymbol{k}}\cdot\hat{\boldsymbol{k}}' \\
C(\boldsymbol{k}) &\equiv \int d\boldsymbol{k}'V(\boldsymbol{k}-\boldsymbol{k}') \\
E(\boldsymbol{k}) &= \sin\varphi_k\,A(\boldsymbol{k}) + \cos\varphi_k\,B(\boldsymbol{k}) \quad (10)
\end{aligned}$$

The H_2^A term in Eq. 9 includes the anomalous combinations of creation and annihilation operators, in other words, terms that would not conserve the number of quark-antiquark pairs (i.e. chiral charge). In order to get rid of H_2^A altogether we set $A(\boldsymbol{k})\cos\varphi_k - B(\boldsymbol{k})\sin\varphi_k = 0$, which is known in the literature as the *Mass Gap equation*.

Finally, H_4 contains the quartic terms coming from the potential and listed in Table 1. These correspond to 10 different types of diagrams. The diagrams which are compatible with mesonic bound states and do not allow to have quarks, or antiquarks in isolation, are shown in Fig. 2. In these diagrams, time flows from left to right, with the arrows going forward in time corresponding to a quark, and those going backward corresponding to an antiquark.

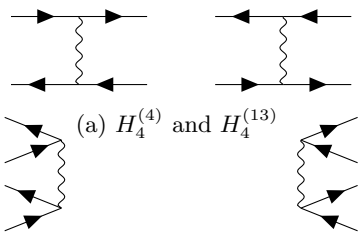

(a) $H_4^{(4)}$ and $H_4^{(13)}$

(b) $H_4^{(6)}$ (c) $H_4^{(11)}$

Figure 2: Diagrammatic representation of the quartic terms listed in Table 1. These terms correspond to color singlets.

	spinor-term	operators	normal ordered
$H_4^{(1)}$	$v_1^+v_2v_3^+v_4$	$D_1D_2^+D_3D_4^+$	$D_2^+D_4^+D_3D_1$
$H_4^{(2)}$	$v_1^+v_2v_3^+u_4$	$D_1D_2^+D_3B_4$	$-D_2^+D_1D_3B_4$
$H_4^{(3)}$	$v_1^+v_2u_3^+v_4$	$D_1D_2^+B_3^+B_4^+$	$-D_2^+B_3^+D_4^+D_1$
$H_4^{(4)}$	$v_1^+v_2u_3^+u_4$	$D_1D_2^+B_3^+B_4$	$-D_2^+B_3^+B_4D_1$
$H_4^{(5)}$	$v_1^+u_2v_3^+v_4$	$D_1B_2D_3D_4^+$	$-D_4^+D_1B_2D_3$
$H_4^{(6)}$	$v_1^+u_2v_3^+u_4$	$D_1B_2D_3B_4$	$D_1B_2D_3B_4$
$H_4^{(7)}$	$v_1^+u_2u_3^+v_4$	$D_1B_2B_3^+D_4^+$	$B_3^+D_4^+D_1B_2$
$H_4^{(8)}$	$v_1^+u_2u_3^+u_4$	$D_1B_2B_3^+B_4$	$B_3^+D_1B_2B_4$
$H_4^{(9)}$	$u_1^+v_2v_3^+v_4$	$B_1^+D_2^+D_3D_4^+$	$-B_1^+D_2^+D_4^+D_3$
$H_4^{(10)}$	$u_1^+v_2v_3^+u_4$	$B_1^+D_2^+D_3B_4$	$B_1^+D_2^+D_3B_4$
$H_4^{(11)}$	$u_1^+v_2u_3^+v_4$	$B_1^+D_2^+B_3^+D_4^+$	$B_1^+D_2^+B_3^+D_4^+$
$H_4^{(12)}$	$u_1^+v_2u_3^+u_4$	$B_1^+D_2^+B_3^+B_4$	$B_1^+D_2^+B_3^+B_4$
$H_4^{(13)}$	$u_1^+u_2v_3^+v_4$	$B_1^+B_2D_3D_4^+$	$-B_1^+D_4^+D_3B_2$
$H_4^{(14)}$	$u_1^+u_2v_3^+u_4$	$B_1^+B_2D_3B_4$	$B_1^+B_2^+D_3B_4$
$H_4^{(15)}$	$u_1^+u_2u_3^+v_4$	$B_1^+B_2B_3^+D_4^+$	$B_1^+B_3^+D_4^+B_2$
$H_4^{(16)}$	$u_1^+u_2u_3^+u_4$	$B_1^+B_2B_3^+B_4$	$B_1^+B_3^+B_4B_2$

Table 1: Quartic operators of the Hamiltonian. In the second column a list of all possible combinations of creation and annihilation operators is shown, together with the corresponding spinor-terms where they do come from (first column). In the last column the same operators are written in their normal ordered form.

3. Hamiltonian and model space

3.1. Effective Hamiltonian

The Hamiltonian we have discussed so far possesses terms where integrals can be approximated by an "average" number term, that preserves the intrinsic fermionic nature. It can be interpreted as a term that creates and annihilates a quark with an average momentum in a given abstract site. For instance:

$$\int d\boldsymbol{k} E(\boldsymbol{k})\, B^\dagger(\boldsymbol{k}) B(\boldsymbol{k}) \approx \sum_n^N E_n B_n^\dagger\, B_n \qquad (11)$$

where we have dropped the flavor and color indices for convenience.

To illustrate this let us consider the simplest possible model ($N = 2$) where:

- One has only two momentum sites, p_I and p_{II}.
- There are fermionic operators A_{ij}, where i refers to the kind of particle, $i = 1, 2$ for quark and anti-quark, respectively; and j to the site, $j = I, II$.

Before proceeding, it is also convenient to establish the following correspondence to other abstract fermionic operators. Since we have 2 species (quark and antiquark) and 2 sites, we need four of them, namely:

$$\begin{aligned} a_1^\dagger &\equiv A_{1,I}^\dagger \qquad & a_1 &\equiv A_{1,I} \\ a_2^\dagger &\equiv A_{1,II}^\dagger \qquad & a_2 &\equiv A_{1,II} \\ a_3^\dagger &\equiv A_{2,II}^\dagger \qquad & a_3 &\equiv A_{2,II} \\ a_4^\dagger &\equiv A_{2,I}^\dagger \qquad & a_4 &\equiv A_{2,I} \end{aligned}$$

A straightforward extension is possible for a denser grid of momenta but, for illustration purposes this is appropriate. The Hamiltonian of this model is:

$$\begin{aligned} H_{\text{eff.}}^{q_1\bar{q}_2} &= H_{\text{const.}} \\ &+ \frac{1}{2} V_{q_1} \left(a_1^\dagger a_1 + a_2^\dagger a_2 \right) + \frac{1}{2} V_{\bar{q}_2} \left(a_4^\dagger a_4 + a_3^\dagger a_3 \right) \\ &+ \frac{1}{2} U \left(a_1^\dagger a_1 a_3^\dagger a_3 + a_2^\dagger a_2 a_4^\dagger a_4 \right) \\ &+ V_b \left(a_1 a_4 a_3 a_2 \right) + V_f \left(a_1^\dagger a_4^\dagger a_3^\dagger a_2^\dagger \right) \end{aligned} \qquad (12)$$

where the first term is just a constant, coming from evaluating H_0 in Eq. 8. The terms with coefficients V_{q_1} and $V_{\bar{q}_2}$ correspond to kinetic terms and one can recast their value (see Eq. 11), but let us for the moment leave them has free parameters of our model.

Similarly, the terms with coefficient U are those obtained from $H_4^{(4)}$ and $H_4^{(13)}$, and depicted in Fig. 2(a), and the terms with coefficient V_b and V_f, from $H_4^{(6)}$ in Fig. 2(b), and $H_4^{(11)}$ in Fig. 2(c).

As explained before there are no other terms for the mesonic sector, which makes Eq. 12 our meson Hamiltonian.

3.2. Fitting strategy to *test* the model and *inspect* the interquark potential

All the coefficients that determine the Hamiltonian in Eq. 12 can be calculated *exactly*. In order to do so, one needs to assume a momentum dependent potential, that describes the underlying physics. This has been done extensively in the literature and will not be repeated here. Instead, our goal is to investigate if *some* properties of such potential can be *unfolded* directly from the measured data, i.e., from the meson mass spectrum.

Our strategy is the following: first, we restrict the analysis only to heavy vector mesons. For simplicity, we normalize the energy units with the mass of the $\phi(1020)$ meson (the lightest vector meson which is not constituted by up or down quarks), so that we get $m_{\phi(1020)} = 1$.

The next step, regardless of being a crude approximation, is to assume the following:

- $H_{\text{const.}} = h_0$ is a constant, chosen so as to guarantee that $V_{\text{cross}} = 0$ for the highest mass ratio, i.e., $m_{\Upsilon(1S)} = h_0$.
- The kinetic terms V_{q_1} and $V_{\bar{q}_2}$ are equal to $m_q/2$, where m_q is the quark and antiquark mass, respectively, estimated as half the mass of the $q\bar{q}$ vector meson in its ground state.
- The interaction term U is the average of the two kinetic terms.

Under these assumptions, we obtain the results in Table 2.

	m	$H_{\text{const.}}$	V_{q_1}	$V_{\bar{q}_2}$	U	V_{cross}
Υ	9.280	9.280	2.320	2.320	2.320	0.000
B_c^*	6.155	9.280	0.759	2.320	1.540	4.919
B_s^*	5.312	9.280	0.250	2.320	1.285	5.571
J/Ψ	3.038	9.280	0.759	0.759	0.759	7.293
D_s^*	2.072	9.280	0.759	0.250	0.505	7.929
ϕ	1.000	9.280	0.250	0.250	0.250	8.647

Table 2: Parameters used for each particle.

These assumptions are justified by what has been previously observed in ref. [4], where a series of different potentials has been considered.

4. Mapping meson onto qubits

4.1. Bravyi-Kitaev transform

The way in which we want to simulate a fermionic system with a quantum computer is by actually emulating the algebra of fermions with the algebra of qubits, effectively mapping the system we want to simulate into the computational objects we can manipulate. Qubits are distinguishable two-level quantum systems which can be described as spin 1/2 particles, however, the electronic system we want to simulate is composed of indistinguishable fermions. The quantum states of these two types of systems are governed by different algebras. While fermions

are described by the algebra

$$\{a_i, a_j^\dagger\} = \delta_{ij}, \qquad \{a_i, a_j\} = \{a_i^\dagger, a_j^\dagger\} = 0, \quad (13)$$

the $SU(2)$ algebra of Pauli spin operators describes spin 1/2 particles.

One possible way to convert fermions into spins is through the Bravyi-Kitaev transform (see [7]), which uses Pauli spin matrices $\sigma^x = X, \sigma^y = Y$ and $\sigma^z = Z$. For this transformation we have:

$$a_1 = \frac{1}{2}(X_1 + iY_1)X_2X_4 \quad a_2 = \frac{1}{2}(Z_1X_2 + iY_2)X_4$$
$$a_3 = \frac{1}{2}Z_2(X_3 + iY_3)X_4 \quad a_4 = \frac{1}{2}(Z_2Z_3X_4 + iY_4) \quad (14)$$

and its hermitian conjugate for the creation operators, which leads to a Hamiltonian equivalent to Eq. 12:

$$\begin{aligned} H_{BK} = H_{\text{const.}} &+ \frac{1}{8}(2(U+2(V_{q_1}+V_{q_2})) \\ &-(U+2V_{q_1})(Z_1+Z_1Z_2) \\ &-(U+2V_{q_2})(Z_3+Z_2Z_3Z_4)+U(Z_1Z_3+Z_1Z_3Z_4) \\ &-V_{\text{cross}}(X_1Z_2X_3+X_1X_3Z_4+X_1Z_2X_3Z_4+X_1X_3) \\ &+V_{\text{cross}}(Y_1Z_2Y_3+Y_1Y_3Z_4+Y_1Z_2Y_3Z_4+Y_1Y_3)) \quad (15) \end{aligned}$$

using $V_b = V_f \equiv V_{\text{cross}}$ for the Hamiltonian to be hermitian.

For this case, only 4 qubits are needed, and the system is simple enough that it can be solved exactly using only a classical computer.

The Hamiltonian will have 16 eigenvalues, and its associated eigenstates (some degenerate). It can be shown that the lowest eigenvalue and its eigenstate is always:

$$\lambda = H_{\text{const.}} + \frac{\beta-\alpha}{2} \quad \begin{matrix}\text{with } \alpha = \sqrt{\beta^2+4V_{\text{cross}}^2} \\ \text{and } \beta = U+V_{q_1}+V_{q_2}\end{matrix} \quad (16)$$

$$|\psi_\lambda\rangle = a\,|0000\rangle + b\,|1010\rangle \quad (17)$$

$$= \frac{\beta+\alpha}{\sqrt{4V_{\text{cross}}^2+(\beta+\alpha)^2}}\,|0000\rangle + \frac{2V_{\text{cross}}}{\sqrt{4V_{\text{cross}}^2+(\beta+\alpha)^2}}\,|1010\rangle \quad (18)$$

where the Dirac notation is in the increasing order $|q_1q_2q_3q_4\rangle$. Note that the Bravyi-Kitaev transform converts the state $|c_1, c_2, c_3, c_4\rangle$ in the Fock basis to the state $|c_1, c_1+c_2, c_3, c_1+c_2+c_3+c_4\rangle \mod 2$, so it converts $|1111\rangle_{\text{Fock}}$ into $|1010\rangle_{BK}$.

Looking at the Hamiltonian expression (Eq. 15), it can be seen that only identity and Z operators, which are diagonal, act on qubits 2 and 4. Since the eigenstate of interest (Eq. 17) is $|0\rangle$ in both of these qubits, then the expected value of qubits 2 and 4's terms is always 1, so they do not contribute to the λ value (Eq. 16).

Therefore these two qubits can be removed (cf. [8]) and the Hamiltonian and eigenstate can be simplified to:

$$\begin{aligned} \tilde{H}_{BK} = H_{\text{const.}} &+ \frac{1}{4}(U+2(V_{q_1}+V_{q_2}) \\ &-(U+2V_{q_1})Z_1-(U+2V_{q_2})Z_3+UZ_1Z_3 \\ &+2V_{\text{cross}}\,(Y_1Y_3-X_1X_3)) \quad (19) \end{aligned}$$

$$|\tilde{\psi_\lambda}\rangle = a\,|00\rangle + b\,|11\rangle \quad (20)$$

Although this simplification could be made thanks to having $|q_2q_4\rangle = |00\rangle$ in Eq. 17, we can see that a Hamiltonian of this type will always be composed solely of I and Z operators in its even indices (with index starting at 1).

The Bravyi-Kitaev transformation doesn't change constant terms ($H_{\text{const.}}$), and converts terms that can be written using solely the number operators (kinetic and interaction terms) into terms composed solely of identity and Z operators (see [9]).

Finally, when using N sites/qubits, it converts the Hamiltonian term $a_Na_{N-1}\dots a_1$ into:

$$\left(\prod_{p\text{ odd}}\frac{X_p+iY_p}{2}\right)\left(\prod_{p\text{ even}}\frac{1+Z_p}{2}\right) \quad (21)$$

The operator $a_N^\dagger a_{N-1}^\dagger \dots a_1^\dagger$ is expectedly similar.

As the cross terms also have the desired property, whenever at least one of the even qubits is $|0\rangle$ or $|1\rangle$ and separable in the eigenstate, it can be simplified out of the Hamiltonian.

5. Quantum computing

For this case, it is possible to calculate, either numerically or even analytically, what is the lowest eigenvalue of the Hamiltonian, and its associated eigenstate, since the number of qubits is low.

However, we may consider the general case of a problem that requires more qubits to be described. If this model described a situation with many coupled particles, then the matrix representing the Hamiltonian would not be sparse and easy to handle, and its size would increase exponentially with the increase in qubits.

With this in mind, below we describe an approach where is it assumed that the eigenvalue and eigenstate (Eqs. 16-18) are not known *a priori*.

A well-established method in quantum chemistry to determine the lowest eigenvalue (and associated eigenstate) of a Hamiltonian using quantum computing is the Variational Quantum Eigensolver (VQE, see [1]). This method requires a Hamiltonian built in terms of Pauli spin matrices, like Eqs. 15 and 19.

5.1. Ansatz

In order to apply this algorithm, it is crucial to have a method to create a quantum state (in a quantum circuit), dependent on some parameters, that we are confident it can generate the eigenstate we

are looking for, for some choice of those parameters. In other words, we wish to have a method (an ansatz) that gives us some unitary transformation $U(\vec{\theta})$ such that $|\psi_\lambda\rangle = U(\vec{\theta})\,|\mathbf{0}\rangle$, for some $\vec{\theta}$. $U(\vec{\theta})$ should restrict *a priori* the number of possible states considerably, by discarding unphysical or unlikely states, in order to be efficient.

Unfortunately, the methods often used in quantum chemistry, like the unitary coupled cluster (see [10]), are only advantageous if the eigenstate differs from a known reference state only by a few electron excitations or relaxations. Here we do not have a good reference state, and we cannot rule out *a priori* the states with many unoccupied or occupied sites (for instance $|1111\rangle$ in the Fock basis). We can only rule out unphysical states, which those methods cannot account for. Therefore, the quantum chemistry methods are not efficient in this case, since if applied they are no better than a method which spans all possible states, and therefore no quantum advantage can be obtained.

Since in this case we are dealing with a simple system, we can deal with the lack of a proper state ansatz in several ways:

- **Entanglement** As we are looking for a solution that represents a meson, we may expect the sought-after eigenstate to be entangled. Any Hamiltonian term that can be written using only number operators $a_i^\dagger a_i$ will either return 0 or the state itself when applied to a state in the Fock basis. Therefore, in matrix form, these terms are located in the diagonal, and cannot lead to entanglement. The remaining terms (cross terms) will only act non-trivially in the vacuum state or the fully occupied state, and only these can lead to entanglement. After the Bravyi-Kitaev transform, our eigenstate will then be Eq. 17.
- **Symmetry** Looking at Eq. 12, we see that certain indices can be swapped without a significant effect on the Hamiltonian. Assuming that a change in the Hamiltonian parameters' values only leads to a change in the probability amplitudes associated with the components of the eigenstate, we can perform any combination of the following index swaps: $\{1 \leftrightarrow 2, 3 \leftrightarrow 4\}$ (site swap), and $\{1 \leftrightarrow 4, 2 \leftrightarrow 3\}$ ($q\bar{q}$ swap); and these swaps should alter the probability amplitudes of the eigenstates' terms, and not the terms themselves. If we consider that the eigenstate must only be a superposition of terms respecting these symmetries, then the only option is for it to be a superposition of $|0000\rangle$ and $|1111\rangle$ (in the Fock basis). After the Bravyi-Kitaev transform, we get Eq. 17.
- **General approach** Presented in detail in Sec. 6. This method can be applied efficiently to most Hamiltonians, in practice.

Since there is not a well-established ansatz for this type of problem, as a case study, we'll consider that we know the eigenstate of interest will be this superposition (using one of the aforementioned methods), but that we don't know the probability amplitudes a and b that constitute it (i.e. we know Eq. 17 but not Eq. 18).

5.2. Quantum circuit

In order to apply the VQE algorithm, we must have a quantum circuit, dependent on some parameters, that is able to create the eigenstate associated with the lowest eigenvalue.

Here the simplified Hamiltonian is used (Eqs. 19 and 20) as it reduces the number of qubits by half. The goal is then to create $|\tilde{\psi_\lambda}\rangle$.

Starting with the state $|00\rangle$, if we apply a R_y rotation by an angle θ, followed by a CNOT gate, we end up with the state:

$$|\tilde{\psi_\lambda}\rangle = \cos\left(\frac{\theta}{2}\right)|00\rangle + \sin\left(\frac{\theta}{2}\right)|11\rangle \tag{22}$$

which can be then implemented by the circuit the Fig. 3.

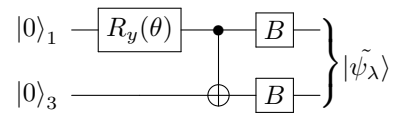

Figure 3: R_y rotation by θ on qubit 1, followed by a CNOT gate, and possibly a B gate, corresponding to a basis change, which is necessary for some Pauli terms in the Hamiltonian (see [10]).

The B gate is equal to H and $HS^\dagger$ for the X_1X_3 and Y_1Y_3 Pauli terms in the Hamiltonian, respectively. The gate is not present for the other terms. H and S correspond to the Hadamard and $R_z(\pi/2)$ gate, respectively.

$$H(a\,|0\rangle + b\,|1\rangle) = a\left(\frac{|0\rangle + |1\rangle}{\sqrt{2}}\right) + b\left(\frac{|0\rangle - |1\rangle}{\sqrt{2}}\right)$$
$$HS^\dagger(a\,|0\rangle + b\,|1\rangle) = a\left(\frac{|0\rangle + |1\rangle}{\sqrt{2}}\right) - ib\left(\frac{|0\rangle - |1\rangle}{\sqrt{2}}\right)$$

Therefore we can create all superpositions of interest of these two states, by an appropriate choice of θ. Note that we assume here that there is no local complex phase. In fact, we know from linear algebra that a hermitian matrix (like this Hamiltonian) with real entries can only have real eigenvalues (which is the energy) and we can always choose real eigenstates (up to a global phase, which is irrelevant).

Here we used two of IBM's publicly available processors (*ibmq_16_melbourne* and *ibmq_ourense*, see [3]) and the Qiskit framework (see [11]) to run the circuit in Fig. 3, being careful to choose the physical qubits and CNOT gate connection available with lowest error rate.

We can then create the quantum state $|\tilde{\psi_\lambda}\rangle$ which will be the desired eigenstate for some choice of the

controllable parameters in our quantum circuit (in our case there is only one, θ).

Since we work with the computational basis (for 2 qubits, that is $\{|00\rangle, |01\rangle, |10\rangle, |11\rangle\}$), when measuring the state $|\tilde{\psi_\lambda}\rangle$ produced, one of the 4 basis states will be measured. Since any of these is an eigenstate for Pauli terms composed with the Z Pauli operator, the expectation value of Z_1, Z_3, Z_1Z_3 can be easily calculated. By producing and measuring $|\tilde{\psi_\lambda}\rangle$ 8192 times, the mean expectation value of each term approximates closely the theoretical expectation value of these terms when applied to $|\tilde{\psi_\lambda}\rangle$. For the X_1X_3 and Y_1Y_3 terms, the B gate must be applied before the measurement, so that the basis states become the eigenstates of these terms (see [12]).

After obtaining these 5 expectation values (equal for all particles), and the coefficients in Table 2 (specific to each particle), we obtain $\langle \tilde{H}_{BK} \rangle \equiv \langle H \rangle$ from Eq. 19, for a certain choice of the initial parameters (in our case, θ). We can then choose some minimization method to determine which are the parameter values that give us the lowest $\langle H \rangle$. Since $\langle H \rangle$ is lower bounded by the ground state energy, then the lowest $\langle H \rangle$ will be the energy of the system, and from our final parameter choice we know the associated eigenstate.

In this case, since only one angle (the parameter θ) is necessary to parametrize the ansatz, the easiest method is to do a parameter scan from $-\pi$ to π (Fig. 4), and then estimate the minimum (Tables 3 and 4).

This approach effectively sidesteps the classical minimization portion of the VQE algorithm, and it is not suitable for more complex problems. As IBM devices have a long waiting queue, it is currently more efficient to send all circuits at once (in a batch) than to send one circuit, with one θ value at a time, wait for the measurement results, and then use the minimizer to choose the next value to send.

If we had many parameters, which required many batches, then the standard minimizer method could be used (or a modified version, which could handle batches). The SPSA algorithm, for example, could be used (see [12]).

5.3. Results

The obtained results are shown in Fig. 4. As the variation of $\langle H \rangle$ is sinusoidal, a cosine fit was used to determine the minimum value of θ, after which the a and b coefficients (Table 3) and meson masses (Table 4) were calculated.

Under the approximation used, where $V_{\text{cross}} \to 0$ for the Υ(1S) meson, the entanglement of the eigenstate practically disappears, as $b \to 0$, and $|\tilde{\psi_\lambda}\rangle = |00\rangle$ which is not entangled. This is to be expected, since the V_{cross} terms of the Hamiltonian are the only off-diagonal terms, and the ones which lead to an entangled eigenstate.

Note that the relative error obtained for a and b is very low for the *ibmq_16_melbourne* device results, despite a noticeable deviation of the mass from the theoretical calculation observed in Fig. 4. It is justified by the robustness of the VQE algorithm when applied to faulty quantum gates. The large mass deviation is mainly due to the amplitude error, which is mostly caused by the $\langle X_1X_3 \rangle$ and $\langle Y_1Y_3 \rangle$ results, that have higher error due to the extra B gate in the circuit (Fig. 3). Since the effect of these two terms is more pronounced for the lower mass particles, the highest mass deviation increases with the decrease of the meson mass.

On the other hand, for the *ibmq_ourense* device results, the masses obtained are closer to the expected value. As it can be seen in the (b) plots in Fig. 4, the deviation of the experimental results from the prediction is about 50% smaller for this device, when compared with *ibmq_16_melbourne*. However, unlike in the larger device, in this case there is a smaller but noticeable phase shift of the results, which leads to the minimum being slightly off its expected position. Looking at the right (c) plot in Fig. 4, it appears that this phase shift is present in nearly all terms of the Hamiltonian. This deviation may then be due to poor device calibration, with the θ angle implemented in the device being slightly different from the angle given by the circuit.

We could also obtain what state $|\tilde{\psi_\lambda}\rangle$ corresponded to initially, in the 2$^{\text{nd}}$ quantization. Reversing the simplification done in Eq. 19 and 20, and reversing the Bravyi-Kitaev transformation, we conclude that the lowest energy eigenstate corresponds to a superposition of the states (in the Fock basis) $|\text{vacuum}\rangle$ and $(A_{1,I}A_{1,II}A_{2,I}A_{2,II} + A^\dagger_{1,I}A^\dagger_{1,II}A^\dagger_{2,I}A^\dagger_{2,II})\,|\text{vacuum}\rangle$, with a and b as the associated amplitudes, respectively.

Therefore, due to our estimated coefficients (Table 2), as the masses of the quarks that compose each meson decrease, the V_{cross} term increases, and the entanglement between the vacuum and the fully occupied state becomes more prominent. This is expected, since in the extreme scenario where $V_{\text{cross}} \to 0$ (Υ(1S) case), the quark and antiquark act as if they are not bounded, and so the vacuum is the lower energy state, and we obtain $|\psi\rangle = |\text{vacuum}\rangle$ using the VQE algorithm. On the other hand, if the quark and antiquark masses are negligible compared to h_0 ($\phi(1020)$ case), so will be their momentum, since we considered the kinetic and interaction coefficients of the Hamiltonian proportional to the quark and antiquark masses, and therefore the binding energy associated with the meson with be similar to the vacuum energy, so the two states will be in superposition, with $a \approx b$, as obtained.

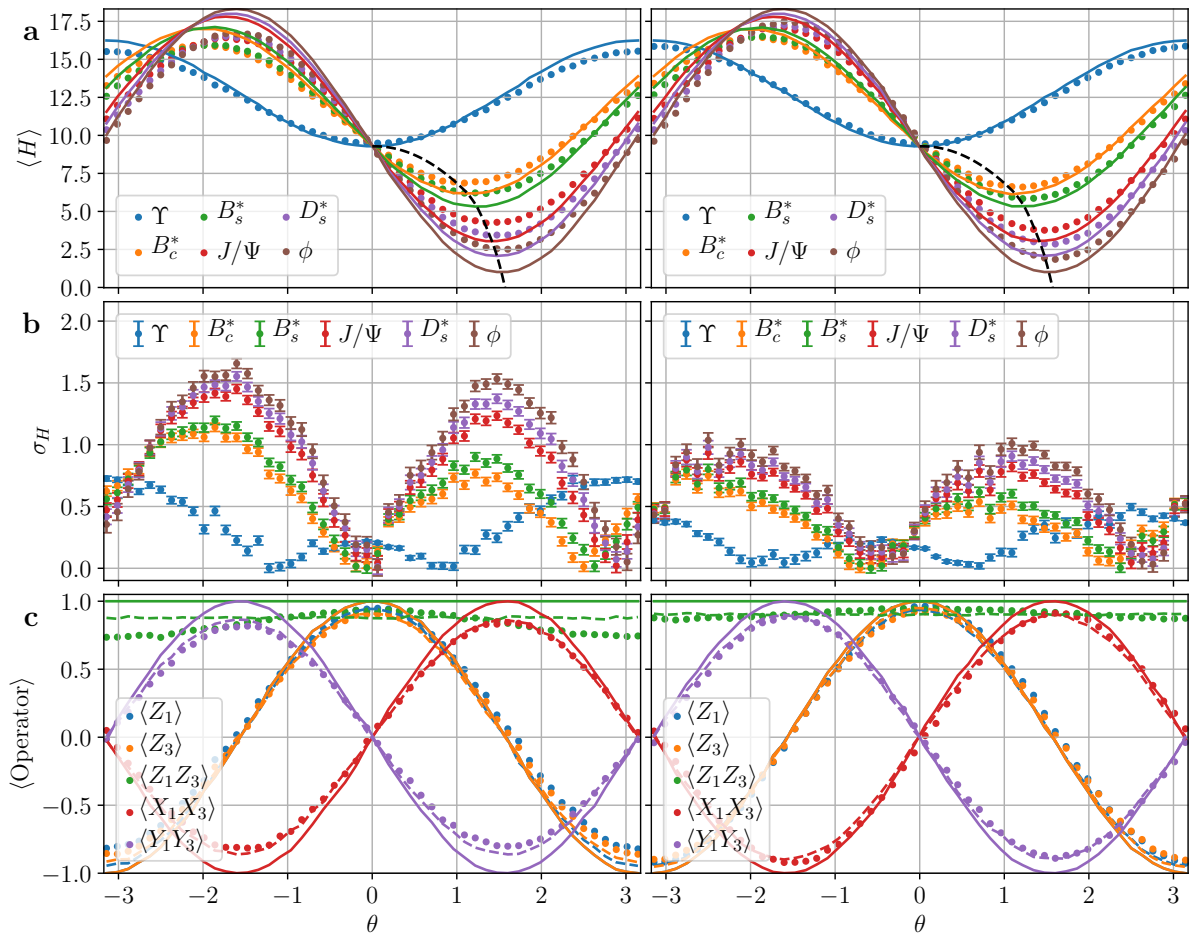

Figure 4: Results obtained using the *ibmq_16_melbourne* (left) and *ibmq_ourense* (right) devices. **(a)** $\langle H \rangle(\theta)$ using the exact solution (lines), and the experimental solution (points), for different particles. The black dashed line roughly indicates the position of the expected minima. **(b)** Deviation from exact result, with errorbars indicating the standard deviation of $\langle H \rangle(\theta)$, associated with the stochasticity of the measured results. **(c)** Comparison of the exact (solid lines) and experimental (points) results of the expected value of each Pauli term composing the Hamiltonian. The deviation can be mostly explained by the effect of quantum device errors (accounted for in dashed lines).

	θ	$a_{\text{theo.}}$	a	$\delta_a(\%)$	$b_{\text{theo.}}$	b	$\delta_b(\%)$
Υ	0.020(13)	1.000	1.000(0)	0.0	0.000	0.010(7)	-
B_c^*	1.127(10)	0.844	0.845(3)	0.2	0.536	0.534(4)	0.4
B_s^*	1.236(10)	0.815	0.815(3)	0.0	0.580	0.580(4)	0.1
J/Ψ	1.422(8)	0.760	0.758(3)	0.3	0.650	0.653(3)	0.4
D_s^*	1.485(8)	0.740	0.737(3)	0.4	0.673	0.676(3)	0.5
ϕ	1.540(7)	0.722	0.718(2)	0.6	0.692	0.696(3)	0.6

	θ	$a_{\text{theo.}}$	a	$\delta_a(\%)$	$b_{\text{theo.}}$	b	$\delta_b(\%)$
Υ	0.053(13)	1.000	1.000(0)	0.0	0.000	0.027(6)	-
B_c^*	1.175(10)	0.844	0.832(3)	1.4	0.536	0.554(4)	3.3
B_s^*	1.283(9)	0.815	0.801(3)	1.6	0.580	0.598(4)	3.2
J/Ψ	1.463(7)	0.760	0.744(2)	2.0	0.650	0.668(3)	2.7
D_s^*	1.524(7)	0.740	0.724(2)	2.2	0.673	0.690(3)	2.6
ϕ	1.578(7)	0.722	0.705(2)	2.4	0.692	0.710(2)	2.6

Table 3: Probability amplitudes for each particle, using *ibmq_16_melbourne* (left) and *ibmq_ourense* (right).

	$m_{\text{theo.}}$	m	$\delta_m(\%)$
Υ	9.280	9.473(40)	2.1
B_c^*	6.155	6.866(48)	11.5
B_s^*	5.312	6.152(48)	15.8
J/Ψ	3.038	4.195(49)	38.1
D_s^*	2.072	3.360(50)	62.2
ϕ	1.000	2.445(50)	144.5

	$m_{\text{theo.}}$	m	$\delta_m(\%)$
Υ	9.280	9.424(41)	1.6
B_c^*	6.155	6.602(48)	7.3
B_s^*	5.312	5.831(48)	9.8
J/Ψ	3.038	3.731(50)	22.8
D_s^*	2.072	2.837(50)	36.9
ϕ	1.000	1.853(51)	85.3

Table 4: Normalized masses for each particle, using *ibmq_16_melbourne* (left) and *ibmq_ourense* (right).

6. General approach

The biggest hindrance to the application of this method for QCD systems is the lack of a good ansatz for state preparation. General catch-all ansätze, which cannot guarantee the creation of the desired eigenstate, but may get close to it, have previously been used (see [12]), but their efficiency is not well studied (see [13]). These system-agnostic methods also require a high number of parameters for an accurate result, as they overparametrize the quantum circuit.

With this problem in mind, it is possible to generalize the entanglement ansatz discussed before, in order to get a decent picture of the eigenstates of a general Hamiltonian.

As we are dealing with fermions, any Hamiltonian expression can be written, by using the fermion commutation rules, so that, for each term, each index i contains one of four possible operators: identity ($\mathbb{1}_i$), annihilation operator (a_i), creation operator ($a_i^\dagger$) and number operator ($n_i \equiv a_i^\dagger a_i$).

Any Hamiltonian can be written in the form:

$$\begin{aligned} H &= H_{\text{const.}} + H_n + H_a \\ H_n &= \sum\nolimits_{\mathbf{i}} b_{i_1 \dots i_N} O_1^{i_1} O_2^{i_2} \dots O_N^{i_N} \\ &\quad \text{for } O^{i_j} \in \{\mathbb{1}, n\}, \text{ excluding constant terms} \\ H_a &= \sum\nolimits_{\mathbf{i}} c_{i_1 \dots i_N} \left(O_1^{i_1} O_2^{i_2} \dots O_N^{i_N} + \text{h.c.}\right) = \sum\nolimits_{\mathbf{i}} H_a^{\mathbf{i}} \\ &\quad \text{for } O^{i_j} \in \left\{\mathbb{1}, a, a^\dagger, n\right\}, \text{ excluding } H_n \text{ terms} \end{aligned} \tag{23}$$

Note that for the $H_{\text{const.}}$ and H_n terms, their eigenstates are the basis states. For the H_a terms, each term will have from 2 (when $\forall i_j : O^{i_j} \notin \{\mathbb{1}\}$) to all (when $\exists_{=1} i_j : O^{i_j} \notin \{\mathbb{1}\}$) eigenstates as a superposition of exactly 2 basis states, with a pair of eigenstates per pair of distinct basis states. All remaining eigenstates will have an associated eigenvalue of zero.

For each term $H_a^{\mathbf{i}}$ in the sum in H_a, let $S^{\mathbf{i}}$ be the set of eigenstates of $H_a^{\mathbf{i}}$ which are not some basis state, and let $B_S^{\mathbf{i}}$ be the set of basis states which are components of at least one state in $S^{\mathbf{i}}$. Let $|b_k\rangle$ be a basis state. Then, there are two possibilities:

- $\exists_{\geq 1} \mathbf{i}$, such that $|b_k\rangle \in B_S^{\mathbf{i}}$. Let V_k be the set of such $\mathbf{i}$. Then, for each $H_a^{\mathbf{i}}, \mathbf{i} \in V_k$ there will be 2 eigenstates of the form $|s_{k,p}\rangle = c_1 |b_k\rangle + c_p |b_p\rangle$, with $|b_p\rangle$ some other basis state. Let D_k^1 be the set of k and of all distinct p present in these superpositions. Let $\mathcal{B}_k^1 \equiv \bigcup_{j \in D_k^1} \{|b_j\rangle\}$, that is, the set of all basis states present. We can analyze these new states $|b_p\rangle$ recursively. Let $D_k^n \equiv \bigcup_{j \in D_k^{n-1}} D_j^1$ and consider $\mathcal{B}_k^n \equiv \bigcup_{j \in D_k^n} \{|b_j\rangle\}$. Then, for some q we must have $\mathcal{B}_k^{q+1} = \mathcal{B}_k^q$ (with the worst case being when $\mathcal{B}_k^q$ contains all basis states). Let $\mathcal{B}_k$ be this final set.
- $\forall \mathbf{i}$, $|b_k\rangle \notin B_S^{\mathbf{i}}$. Then $|b_k\rangle$ is an eigenstate of H_a, with eigenvalue of zero. We define in this case $\mathcal{B}_k \equiv \{|b_k\rangle\}$.

We may then conclude that any state in $\mathcal{B}_k$ may only be in a superposition with states in this set. If $|b_z\rangle \notin \mathcal{B}_k$ were to be in a superposition with some state $|b_l\rangle \in \mathcal{B}_k$, then there would have to be some term $H_a^{\mathbf{i}}$ such that a superposition of $|b_z\rangle$ and some state in $\mathcal{B}_k$ was its eigenstate. But if that were the case, then $|b_z\rangle$ would be in $\mathcal{B}_k$, which is a contradiction. We conclude that a superposition of some or all states in $\mathcal{B}_k$ must be an eigenstate of H_a. As H_a is hermitian, then its eigenstates must be orthogonal, and thus, if $\mathcal{B}_k$ contains K states, these states must compose K eigenstates.

If $|r\rangle = \sum a_k |b_k\rangle$ is an eigenstate of H_a, then, since every state is an eigenstate of $H_{\text{const.}}$; and H_n is a diagonal operator, that is, $H_n |b_k\rangle = c_k |b_k\rangle$, we conclude that $|r'\rangle = \sum a'_k |b_k\rangle$ (where a'_k may be zero) is an eigenstate of H.

We can then effectively divide the basis states into distinct $\mathcal{B}_k$ sets, with all the eigenstates of H_a and H being a superposition of the states in each $\mathcal{B}_k$ set.

If we represent the eigenstates using a graph, where the nodes are basis states and the edges connect states which compose an eigenstate of $H_a^{\mathbf{i}}$ (for some $\mathbf{i}$), then the maximally connected subgraph containing the initial state $|b_k\rangle$ will have the states in $\mathcal{B}_k$ as its nodes.

We now present an efficient way of determining the $\mathcal{B}_k$ sets, and the exact edges present in the graph representation. Only the terms in H_a need to be addressed, and for each term it is not necessary to consider the hermitian conjugate component, since we know that if one term transforms state $|i\rangle$ into state $|f\rangle$, then its hermitian conjugate will do the opposite transformation. For these relevant terms:

A: If index i contains a_i or $a_i^\dagger$, then the superposition is of the form $c_0 |0_i\rangle + c_1 |1_i\rangle$ for that index, with the graph edge being $|0_i\rangle \leftrightarrow |1_i\rangle$;

B: If it contains n_i, then we have $|1_i\rangle \leftrightarrow |1_i\rangle$;

C: If index i is not present, then we get $|f_i\rangle \leftrightarrow |f_i\rangle$, with f equal to 0 or 1;

D: In all other cases, the term can be rewritten, using fermionic commutation rules, to fall into one of the previous cases.

For example, considering 4 total sites, the term $a_1 a_4 a_2^\dagger a_2$ will lead to the two edges $|0_1 1_2 f_3 0_4\rangle \leftrightarrow |1_1 1_2 f_3 1_4\rangle$ and the two superpositions $c_1 |0_1 1_2 f_3 0_4\rangle + c_2 |1_1 1_2 f_3 1_4\rangle$, one for $f = 0$ and one for $f = 1$.

It is not necessary to order the indices of the operators in case D, since reordering indices adds at most a minus sign to the term (according to fermionic commutation rules). Since the probability amplitudes of each component in the superposition eigenstates are not known *a priori*, without costly computation, then this minus sign will simply affect these unknown amplitudes, and thus it is not worth accounting for.

In the general case, if we have M unique terms in our total Hamiltonian H, between 0 and $M/2$ terms will need to be analyzed in this manner. Each analyzed term will correspond to 2^k edges, where the term has k indices in case C.

Note that this analysis can only be efficiently done using the Hamiltonian in second quantization and the Fock basis, since it is more likely for this Hamiltonian to contain terms which affect different basis states non-trivially, and for terms to be linearly independent (with each term having a distinct coefficient). If the Hamiltonian expression diverges significantly from these assumptions, them the analysis will overestimate superposition between states composing the eigenstates, thereby reducing its usefulness.

By knowing the possible superpositions, we can then restrict the search space significantly, and create an efficient quantum circuit. This circuit can be built by modifying the algorithm for a general state, or by trying to group together simpler circuits that create each eigenstate of interest separately.

7. Summary and conclusions

In this work, we have showcased that it is possible to use local fermionic modes acting on the abstract qubit Fock space in very complex problems and still gain a new perspective.

Results close to the theoretical prediction were obtained despite the significant physical errors still present in current publicly available quantum computers. All the results obtained required a minimal number of runs in the quantum circuit. In fact, as the Hamiltonians associated with each particle were similar, the quantum results could be reused, and a total of $N_{\text{circuits}} \times N_\theta \times N_{\text{runs}} = 3 \times 50 \times 8192$ runs were made, for the results shown. The associated errors were also significantly reduced by removing half of used qubits, which were redundant. This minimization, both in the number of quantum circuit runs and in number of qubits, could prove useful for implementations of the VQE algorithm to physical problems.

As the approaches used to formulate the quantum circuit for quantum chemistry problems are not useful in this context, the new approach here presented, based on entanglement and symmetry considerations, could work for other physical systems without a proper circuit ansatz. For more complex systems, the general approach introduced could lead to a usable and efficient quantum circuit.

In the future, this work could be expanded to include more momentum sites, in order to explore the differences with this simplest model and study the entanglement pattern. A more complex momentum site also poses a more challenging quantum simulation problem, as the number of necessary qubits scales proportionately, further justifying the use of quantum computation. In this case, a phenomenological interquark potential would have to be assumed, as no easy fitting scheme is possible. It is also feasible to explore this approach with other quark composite systems, such as baryons and possibly tetraquarks.

Although currently not feasible with real quantum hardware, the VQE implementation here presented could be combined with quantum error correction to study how the error rates are affected, and how much these can be reduced. As the newer quantum devices provide lower and lower overall error rates, this approach could provide results with an accuracy similar to that obtainable with traditional classical computation approaches.

References

[1] A. Peruzzo *et al.*, Nature Communications **5**, 4213 (2014).

[2] T. Byrnes and Y. Yamamoto, Physical Review A **73**, 022328 (2006).

[3] IBM Q Experience website, https://quantum-computing.ibm.com.

[4] P. J. d. A. Bicudo and J. E. F. T. Ribeiro, Phys. Rev. **D42**, 1611 (1990).

[5] A. Le Yaouanc, L. Oliver, O. Pene, and J.-C. Raynal, Phys.l Rev. D **29**, 1233 (1984).

[6] A. Le Yaouanc, L. Oliver, S. Ono, O. Pene, and J.-C. Raynal, Physical Review D **31**, 137 (1985).

[7] A. Tranter *et al.*, International Journal of Quantum Chemistry **115**, 1431 (2015).

[8] P. O'Malley *et al.*, Physical Review X **6**, 031007 (2016).

[9] J. T. Seeley, M. J. Richard, and P. J. Love, The Journal of Chemical Physics **137**, 224109 (2012).

[10] J. R. McClean, J. Romero, R. Babbush, and A. Aspuru-Guzik, New Journal of Physics **18**, 023023 (2016).

[11] Open source quantum information science kit website, https://qiskit.org/.

[12] A. Kandala *et al.*, Nature **549**, 242 (2017).

[13] Q. Gao *et al.*, Computational investigations of the lithium superoxide dimer rearrangement on noisy quantum devices, 2019, arXiv: 1906.10675.